*Acta Cryst.* (1996). B52, 810–816

# Structures of Room-Temperature and Ferroelectric (35 K) Phases of Deuterated Betaine Calcium Chloride Dihydrate

J. M. EZPELETA,[a] F. J. ZÚÑIGA,[a] W. PAULUS,[b] A. COUSSON,[b] J. HLINKA[b] AND M. QUILICHINI[b]

[a]*Departamento de Física de la Materia Condensada, Facultad de Ciencias, Universidad del País Vasco, Apdo 644, 48080 Bilbao, Spain, and* [b]*Laboratoire Léon Brillouin, CEN-Saclay, Gif-sur-Yvette 91191 CÉDEX, France. E-mail: wmpezarj@lg.ehu.es*

(*Received 15 August 1995; accepted 20 November 1995*)

## Abstract

The structures of the room-temperature and the lowest-temperature ferroelectric phases of fully deuterated betaine (trimethylammonioacetate) calcium chloride dihydrate have been determined by means of elastic neutron diffraction. In previous structural studies the structural distortions of the incommensurate phase at 130 K and the fourfold phase at 90 K were analyzed in terms of symmetry modes. The same approach has been applied in the present case and, as a result, a quantitative comparison of the distortions at different temperatures can be performed. This shows that the $\Lambda_3$ (for $q \neq 0$) and $B_{2u}$ (for $q = 0$) modes, corresponding to the order parameter, are predominant for the three phases. In addition, it has been found that the structure of this primary mode remains essentially unaltered in the three phases. There is only an increase in its global amplitude as the temperature decreases. Accordingly, it can be expected that the structures of the remaining intermediate modulated phases in the transition sequence are similar to that of the first incommensurate phase, except for the change of wavevector values and greater amplitude of the distortion. Crystal data: $(CD_3)_3NCD_2COOCaCl_2.2D_2O$, $M_r = 279.0$, $\lambda = 0.8308$ Å, $Z = 4$, $F(000) = 552$. At room temperature: *Pnma*, $a = 10.95(1)$, $b = 10.15(1)$, $c = 10.82(1)$ Å, $V = 1203(2)$ Å$^3$, $D_x = 1.54$ g cm$^{-3}$, $\mu = 0.10$ cm$^{-1}$, final $R = 0.048$ for 748 unique observed reflections. At 35 K: $Pn2_1a$, $a = 10.905(9)$, $b = 10.00(1)$, $c = 10.80(1)$ Å, $V = 1178(2)$ Å$^3$, $D_x = 1.57$ g cm$^{-3}$, $\mu = 0.11$ cm$^{-1}$, final $R = 0.042$ for 1726 unique observed reflections.

## 1. Introduction

Betaine calcium chloride dihydrate (BCCD and DBCCD for the deuterated homolog) exhibits a long sequence of phase transitions leading to many commensurate and incommensurate (INC) phases, which correspond to modulations along the $c$ axis of an underlying basic structure with *Pnma* symmetry. X-ray and neutron diffraction studies of the modulation wavevector $\mathbf{q} = \delta\mathbf{c}^*$ provided clear evidence of the INC or commensurate character of those phases with a larger temperature stability range. A first transition at 164 K leads to an INC phase ($\delta$ varying from 0.320 to 0.285), followed by a commensurate ($\delta = 2/7$), a second INC ($0.285 < \delta < 0.25$) and three commensurate phases with $\delta = 1/4$, 1/5 and 0 (Brill & Ehses, 1985). Additional phases, stable in very narrow temperature ranges and sandwiched between the previous phases, were detected by dielectric and pyroelectric measurements and assigned, by means of symmetry arguments, to high-order modulated commensurate phases (in general, termed as $m$-fold phase when $\delta = n/m$). Some of these phases were confirmed by diffraction techniques later and now more than 15 different phases between 164 and 46 K have been established. Besides this, bias electric field and pressure may induce new phases and enlarge the stability temperature range of the high-order commensurate phases. Table 1 gives a summary of the modulation wavevector and transition

Table 1. *Phase sequence in BCCD and DBCCD according to available experimental data*

Column 1: wavevector of the modulation $\mathbf{q} = \delta\mathbf{c}^*$. Column 2: temperature range of stability of the corresponding phases of BCCD according to dielectric data in Unruh, Hero & Dvorak (1989). Column 3: temperature range of stability of DBCCD according to Almeida, Chaves, Kiat, Schneck, Schwarz, Toledano, Ribeiro, Klopperpieper, Muser & Albers (1992). Column 4: (super)space group of the corresponding phases determined by diffraction methods.

| $\delta$ | Transition temperatures (K) | | (Super)space group |
|---|---|---|---|
| 0/1 | Above 164.0 | Above 164 | *Pnma* |
| $\delta > 2/7$ | 164.0–127.8 | 164–130 | $P(Pnma) : 1s\bar{1}$ |
| 2/7 | 127.8–124.5 | 130–127 | |
| $3/11 < \delta < 2/7$ | 124.5–118.4 | | |
| 3/11 | 118.4–117.4 | | |
| $4/15 < \delta < 3/11$ | 117.4–116.0 | | |
| 4/15 | 116.0–115.7 | | |
| $1/4 < \delta < 4/15$ | 115.7–115.4 | | |
| 1/4 | 115.4–75.8 | 117–80 | $P2_1ca$ |
| 2/9 | 75.8–75.2 | 80–79.4 | |
| $1/5 < \delta < 2/9$ | | 79.4–78.5 | |
| 1/5 | 75.2–53.3 | 78.5–57 | |
| 2/11 | 53.3–53.0 | | |
| 1/6 | 53.0–47.1 | 56–50 | |
| 2/13 | 47.1–46.9 | | |
| 1/7 | 46.9–46.2 | | |
| 1/8 | 46.2–46.0 | | |
| 0/1 | 46.0 and below | 50 and below | $Pn2_1a$ |

Table 2. *Experimental details*

| | 293 K | 35 K |
|---|---|---|
| **Crystal data** | | |
| Chemical formula | $C_5D_{15}CaCl_2NO_4$ | $C_5D_{15}CaCl_2NO_4$ |
| Chemical formula weight | 279.0 | 279.0 |
| Cell setting | Orthorhombic | Orthorhombic |
| Space group | *Pnma* | $Pn2_1a$ |
| $a$ (Å) | 10.95 (1) | 10.905 (9) |
| $b$ (Å) | 10.15 (1) | 10.00 (1) |
| $c$ (Å) | 10.82 (1) | 10.80 (1) |
| $V$ (Å$^3$) | 1203 (2) | 1178 (2) |
| $Z$ | 4 | 4 |
| $D_x$ (Mg m$^{-3}$) | 1.54 | 1.57 |
| Radiation type | Neutron | Neutron |
| Wavelength (Å) | 0.8308 | 0.8308 |
| No. of reflections for cell parameters | 22 | 22 |
| $\theta$ range (°) | 15–35 | 15–40 |
| $\mu$ (mm$^{-1}$) | 0.01 | 0.011 |
| Temperature (K) | 293 | 35 |
| Crystal form | Cube | Cube |
| Crystal size (mm) | 3.5 × 3.5 × 3.5 | 3.5 × 3.5 × 3.5 |
| Crystal color | Colorless | Colorless |
| **Data collection** | | |
| Diffractometer | 5C2 four-circle | 5C2 four-circle |
| Monochromator | Cu (420) | Cu (420) |
| $(\sin\theta/\lambda)_{max}$ (Å$^{-1}$) | 0.7300 | 0.7744 |
| Data collection method | $\omega$ | $\omega$ |
| $\omega$ scan width | 7–27tan $\theta$ + 45tan$^2$ $\theta$ | 7–27tan $\theta$ + 45tan$^2$ $\theta$ |
| Absorption correction | None | None |
| No. of measured reflections | 3069 | 2610 |
| No. of independent reflections | 979 | 2019 |
| No. of observed reflections | 748 | 1726 |
| Criterion for observed reflections | $I > 3\sigma(I)$ | $I > 3\sigma(I)$ |
| $R_{int}$ | 0.035 | 0.028 |
| $\theta_{max}$ (°) | 37.34 | 40.04 |
| Range of $h$, $k$, $l$ | $-16 \rightarrow h \rightarrow 16$<br>$0 \rightarrow k \rightarrow 14$<br>$-15 \rightarrow l \rightarrow 15$ | $-16 \rightarrow h \rightarrow 16$<br>$0 \rightarrow k \rightarrow 15$<br>$-15 \rightarrow l \rightarrow 15$ |
| No. of standard reflections | 3 | 3 |
| Frequency of standard reflections (min) | 60 | 60 |
| Intensity decay (%) | 2 | 3.5 |
| **Refinement** | | |
| Refinement on | $F$ | $F$ |
| $R$ | 0.048 | 0.042 |
| $wR$ | 0.047 | 0.042 |
| $S$ | 3.53 | 3.76 |
| No. of reflections used in refinement | 838 | 1902 |
| No. of parameters used | 140 | 255 |
| H-atom treatment | All H-atom parameters refined | All H-atom parameters refined |
| Weighting scheme | $w = 1/\sigma^2(F)$ | $w = 1/\sigma^2(F)$ |
| $(\Delta/\sigma)_{max}$ | 0.16 | 0.68 |
| $\Delta\rho_{max}$ (e Å$^{-3}$) | 1.06 | 1.11 |
| $\Delta\rho_{min}$ (e Å$^{-3}$) | −0.89 | −0.94 |
| Extinction method | Type I, Lorentzian | Type I, Lorentzian |
| Extinction coefficient | 0.108 (6) × $10^3$ | 0.60 (2) × $10^1$ |
| Source of atomic scattering factors | Sears (1992) | Sears (1992) |

temperature of the different phases of BCCD and reference to the above results may be found in the more recent works of Chaves, Kiat, Schwarz, Schneck, Almeida, Klopperpieper, Muser & Albers (1993), Chaves, Almeida, Toledano, Schneck, Kiat, Schwarz, Ribeiro, Klopperpieper, Albers & Muser (1993) and references therein.

The structural details of the INC and fourfold modulated phases have been analyzed by means of X-ray diffraction (Zúñiga, Ezpeleta, Pérez-Mato, Paciorek & Madariaga, 1991; Ezpeleta, Zúñiga, Pérez-Mato, Paciorek & Breczewski, 1992). The structural distortion of the INC phase corresponds to a sinusoidal modulation with amplitudes ranging from 0.03 Å for the Cl atom up to 0.36 Å for the C2 atom. These amplitudes increase in the fourfold modulated phase at lower temperature, but their phases have approximately the same values. Another interesting feature of these structures is the rigid-body behavior of some parts of the BCCD molecule. In both studied phases the structural atomic distortion of atoms C1, N, C2, C2′ and C3 (C2′ symmetry related to C2), forming the betaine molecule, is well described by rigid-body rotations and translations of the group and, although

Table 3. *Fractional atomic coordinates and equivalent isotropic displacement parameters (Å²) for DBCCD*

$U_{eq} = (1/3)\sum_i\sum_j U_{ij}a_i^*a_j^*\mathbf{a}_i.\mathbf{a}_j.$

| | $x$ | $y$ | $z$ | $U_{eq}$ |
|---|---|---|---|---|
| 35 K | | | | |
| Ca | 0.1931 (4) | 0.2358 (4) | 0.2251 (3) | 0.005 (1) |
| Cl1 | 0.3157 (2) | 0.4227 (2) | 0.0869 (2) | 0.0054 (5) |
| Cl2 | 0.2915 (2) | 0.0284 (2) | 0.0889 (2) | 0.0056 (5) |
| O31 | 0.0994 (4) | 0.4126 (4) | 0.3386 (3) | 0.007 (1) |
| O32 | 0.0794 (4) | 0.0965 (4) | 0.3595 (3) | 0.006 (1) |
| O2 | 0.3354 (4) | 0.2093 (4) | 0.3751 (3) | 0.0084 (9) |
| O1 | 0.5345 (4) | 0.2346 (4) | 0.4124 (3) | 0.0059 (9) |
| C4 | 0.4257 (3) | 0.2236 (3) | 0.4445 (2) | 0.0036 (7) |
| C3 | 0.3911 (3) | 0.2239 (3) | 0.5815 (2) | 0.0044 (7) |
| N | 0.4923 (2) | 0.2564 (2) | 0.6727 (2) | 0.0050 (5) |
| C1 | 0.4339 (4) | 0.2622 (4) | 0.7991 (3) | 0.0080 (9) |
| C21 | 0.5477 (4) | 0.3905 (3) | 0.6447 (3) | 0.0076 (9) |
| C22 | 0.5881 (4) | 0.1501 (4) | 0.6737 (3) | 0.0091 (9) |
| D11 | 0.3658 (5) | 0.3408 (4) | 0.7996 (4) | 0.020 (1) |
| D12 | 0.3943 (5) | 0.1656 (4) | 0.8191 (4) | 0.020 (1) |
| D2 | 0.5048 (5) | 0.2874 (4) | 0.8661 (3) | 0.022 (1) |
| D31 | 0.6082 (5) | 0.4171 (5) | 0.7209 (4) | 0.023 (1) |
| D32 | 0.6523 (5) | 0.1736 (5) | 0.7485 (4) | 0.026 (2) |
| D41 | 0.4744 (5) | 0.4637 (4) | 0.6380 (4) | 0.022 (1) |
| D42 | 0.5453 (5) | 0.0547 (4) | 0.6914 (4) | 0.024 (2) |
| D51 | 0.5990 (5) | 0.3839 (4) | 0.5585 (4) | 0.019 (1) |
| D52 | 0.6340 (4) | 0.1479 (4) | 0.5844 (3) | 0.020 (1) |
| D61 | 0.3202 (5) | 0.3000 (4) | 0.5948 (4) | 0.021 (1) |
| D62 | 0.3543 (5) | 0.1259 (4) | 0.6059 (4) | 0.022 (1) |
| D71 | 0.0125 (6) | 0.4054 (5) | 0.3597 (5) | 0.031 (2) |
| D72 | −0.0081 (6) | 0.0855 (5) | 0.3714 (5) | 0.030 (2) |
| D81 | 0.1373 (5) | 0.4449 (5) | 0.4138 (5) | 0.029 (2) |
| D82 | 0.1163 (5) | 0.0540 (5) | 0.4310 (4) | 0.030 (2) |
| 293 K | | | | |
| Ca | 0.1954 (4) | 1/4 | 0.2245 (4) | 0.028 (1) |
| Cl | 0.3040 (2) | 0.4465 (2) | 0.0878 (2) | 0.0399 (6) |
| O3 | 0.0899 (4) | 0.4051 (4) | 0.3491 (4) | 0.052 (1) |
| O2 | 0.3418 (5) | 1/4 | 0.3679 (5) | 0.063 (2) |
| O1 | 0.5359 (4) | 1/4 | 0.4120 (4) | 0.042 (2) |
| C4 | 0.4281 (3) | 1/4 | 0.4402 (3) | 0.028 (1) |
| C3 | 0.3891 (3) | 1/4 | 0.5749 (4) | 0.029 (1) |
| N | 0.4864 (2) | 1/4 | 0.6702 (2) | 0.041 (1) |
| C1 | 0.4262 (7) | 1/4 | 0.7934 (5) | 0.068 (3) |
| C2 | 0.5622 (5) | 0.3716 (7) | 0.6582 (5) | 0.093 (2) |
| D1 | 0.3694 (3) | 0.3353 (6) | 0.8029 (4) | 0.090 (2) |
| D2 | 0.4917 (9) | 1/4 | 0.8624 (7) | 0.145 (5) |
| D3 | 0.6209 (6) | 0.374 (1) | 0.7376 (6) | 0.176 (4) |
| D4 | 0.5029 (6) | 0.4530 (7) | 0.6631 (8) | 0.150 (4) |
| D5 | 0.6139 (4) | 0.3662 (6) | 0.5759 (5) | 0.107 (2) |
| D6 | 0.3330 (4) | 0.3350 (5) | 0.5912 (4) | 0.081 (2) |
| D7 | 0.0044 (4) | 0.4065 (5) | 0.3657 (4) | 0.070 (2) |
| D8 | 0.1270 (4) | 0.4442 (5) | 0.4211 (4) | 0.069 (1) |

worse results are obtained for the same fitting with the Ca octahedra, the suggestion from TLS analysis that correlated librations of the betaine molecules and Ca octahedra are critical degrees of freedom of the phase transitions is still open.

Many theoretical works have also been devoted to the study of this compound under two different approaches: phenomenological models based on Landau expansions (Ribeiro, Tolédano, Chaves, Almeida, Muser, Albers & Klopperpieper, 1990) and Ising-type microscopic models (Tentrup & Siems, 1990). Using the Landau theory and based on the existence of a single symmetry-breaking order parameter with $\Lambda_3$ symmetry, Pérez-Mato (1988) succeeded to explain the whole sequence of phase transitions and predict possible space groups for many commensurate phases. Under the same approach, Dvorák (1990) proposed a more complex mechanism involving two symmetry-breaking order parameters of $\Lambda_3$ and $\Lambda_2$ symmetry, the onset of the second taking place at low temperature (Almeida, Chaves, Kiat, Schneck, Schwarz, Toledano, Ribeiro, Klopperpieper, Muser & Albers, 1992). In terms of these models the structure of the whole series of phases can be considered as small distortions of the basic structure above 164 K, with orthorhombic *Pnma* symmetry (Brill, Schildkamp & Spilker, 1985). Accordingly, the main structural modulation should correspond to a $\Lambda_3$ or $\Lambda_3 + \Lambda_2$ distortion, for the former and second models, respectively. In this way the structural analysis of the INC phase at 130 K and the fourfold phase at 90 K point to a single-order parameter model, although the other model is not discarded. The INC structure was refined under the superspace group $P(Pnma)$:$1s\bar{1}$, which implies that the first harmonic of the distortion has $\Lambda_3$ symmetry and other refinements, with superspace groups compatible with the two-order parameters model, did not improve the results but doubled the number of refined parameters. In the case of the fourfold phase, both models predict the same symmetry. However, the structural analysis of this phase shows that the $\Lambda_2$ distortion is much less relevant than the $\Lambda_3$ distortion, corresponding to the role of secondary and primary order parameters, respectively. On the other hand, it has been found that the structure of the modulated fourfold phase is essentially the same as that of the INC phase with a major contribution of the $\Lambda_3$ mode to the distortion. An extrapolation of this result at lower temperatures implies similar structures for the successive phases, with greater amplitudes of the distortion and the corresponding changes of the wavevector.

In this paper we report the structures of the room temperature and ferroelectric lowest temperature phase ($T < 45$ K) of DBCCD, which exhibits the same sequence of transitions as BCCD but with transition temperatures shifted by a few degrees. The structural distortion at 35 K is analyzed in terms of symmetry modes and compared with the distortions of the INC and fourfold phases of BCCD at 130 and 90 K, respectively.

## 2. Structure determinations

To collect the neutron diffraction intensities a colorless cube-shaped crystal was mounted on the 5C2 four-circle diffractometer at the ORPHEE reactor (Saclay, France). A summary of the crystal data and data collection parameters is given in Table 2.

For reduction of the data to $|F|$ moduli and refinement of the structures, the *XRAY*72 system of programs (Stewart, Kruger, Ammon, Dickinson & Hall, 1972) was used. The source of scattering lengths was from Sears (1992).

Table 4. *Interatomic distances (Å) and angles (°) of DBCCD at room temperature and 35 K*

| | 35 K | 293 K |
|---|---|---|
| Ca—O2 | 2.258 (6) | 2.233 (7) |
| Ca—O1$^{i}$ | 2.280 (6) | 2.289 (6) |
| Ca—O31 | 2.381 (6) | 2.374 (6) |
| Ca—O32 | 2.363 (6) | 2.374 (6) |
| Ca—Cl1 | 2.740 (5) | 2.754 (4) |
| Ca—Cl2 | 2.759 (5) | 2.754 (4) |
| Cl1—Cl2 | 3.952 (3) | 3.988 (3) |
| O31—Cl1 | 3.600 (5) | 3.700 (5) |
| O32—Cl2 | 3.788 (5) | 3.700 (5) |
| O31—O32 | 3.176 (6) | 3.149 (6) |
| O31—D71 | 0.977 (8) | 0.955 (6) |
| O31—D81 | 0.967 (6) | 0.964 (6) |
| O32—D72 | 0.968 (8) | 0.955 (6) |
| O32—D82 | 0.969 (6) | 0.964 (6) |
| C4—O2 | 1.246 (5) | 1.229 (6) |
| C4—O1 | 1.240 (5) | 1.221 (5) |
| C4—C3 | 1.526 (4) | 1.519 (5) |
| C3—D61 | 1.094 (6) | 1.075 (5) |
| C3—D62 | 1.092 (5) | 1.075 (5) |
| C3—N | 1.514 (4) | 1.484 (5) |
| N—C21 | 1.502 (4) | 1.494 (7) |
| N—C22 | 1.491 (4) | 1.494 (7) |
| C1—D11 | 1.082 (6) | 1.072 (7) |
| C1—D12 | 1.080 (6) | 1.072 (7) |
| C1—D2 | 1.088 (6) | 1.036 (9) |
| C1—N | 1.507 (4) | 1.487 (7) |
| C21—D31 | 1.088 (6) | 1.074 (8) |
| C21—D41 | 1.086 (6) | 1.052 (9) |
| C21—D51 | 1.087 (5) | 1.058 (7) |
| C22—D32 | 1.094 (6) | 1.074 (8) |
| C22—D42 | 1.079 (6) | 1.052 (9) |
| C22—D52 | 1.086 (5) | 1.058 (7) |
| | | |
| O2—Ca—O31 | 90.8 (2) | 87.5 (2) |
| O2—Ca—O32 | 81.4 (2) | 87.5 (2) |
| O2—Ca—Cl1 | 97.8 (2) | 93.6 (2) |
| O2—Ca—Cl2 | 91.5 (2) | 93.6 (2) |
| O31—Ca—O32 | 84.1 (2) | 83.1 (2) |
| O31—Ca—Cl1 | 89.0 (2) | 92.0 (1) |
| O31—Ca—Cl2 | 177.4 (2) | 175.0 (2) |
| O32—Ca—Cl2 | 95.1 (2) | 92.0 (1) |
| O32—Ca—Cl1 | 173.0 (2) | 175.0 (2) |
| Cl1—Ca—Cl2 | 91.9 (1) | 92.8 (2) |
| D71—O31—D81 | 104.1 (6) | 104.9 (5) |
| D72—O32—D82 | 104.7 (6) | 104.9 (5) |
| Ca—O2—C4 | 163.9 (3) | 175.5 (3) |
| O2—C4—O1 | 126.8 (3) | 125.9 (4) |
| O2—C4—C3 | 112.8 (3) | 113.2 (4) |
| O1—C4—C3 | 120.4 (3) | 120.9 (4) |
| D61—C3—D62 | 109.4 (4) | 106.9 (4) |
| D61—C3—N | 106.3 (3) | 107.3 (3) |
| D62—C3—N | 107.7 (3) | 107.3 (3) |
| D61—C3—C4 | 107.7 (3) | 108.6 (3) |
| D62—C3—C4 | 108.9 (3) | 108.6 (3) |
| N—C3—C4 | 116.8 (3) | 117.6 (3) |
| C21—N—C22 | 110.9 (3) | 111.4 (4) |
| C21—N—C3 | 110.7 (2) | 109.9 (3) |
| C22—N—C3 | 111.2 (2) | 109.9 (3) |
| C21—N—C1 | 108.6 (2) | 109.0 (3) |
| C22—N—C1 | 108.5 (2) | 109.0 (3) |
| C3—N—C1 | 106.8 (2) | 107.7 (3) |
| D11—C1—D12 | 112.0 (5) | 107.8 (8) |
| D11—C1—D2 | 108.5 (4) | 109.5 (5) |
| D12—C1—D2 | 111.0 (4) | 109.5 (5) |
| D11—C1—N | 108.8 (3) | 110.1 (4) |
| D12—C1—N | 108.4 (3) | 110.1 (4) |
| D2—C1—N | 108.1 (4) | 109.8 (7) |
| D51—C21—D31 | 110.5 (5) | 110.7 (7) |
| D51—C21—D41 | 111.3 (4) | 114.5 (8) |
| D31—C21—D41 | 109.4 (4) | 108.4 (9) |
| D52—C22—D32 | 111.4 (5) | 110.7 (7) |
| D52—C22—D42 | 109.8 (4) | 114.5 (8) |
| D32—C22—D42 | 109.7 (5) | 108.4 (9) |

Symmetry code: (i) $x-\frac{1}{2}, y, \frac{1}{2}-z$ at 35 K; $x-\frac{1}{2}, \frac{1}{2}-y, \frac{1}{2}-z$ at 293 K.

The room-temperature structure was refined using as a starting structural model that of BCCD determined by X-ray diffraction at the same temperature (Brill, Schildkamp & Spilker, 1985). For the low-temperature structure, the $Pn2_1a$ space group predicted by Pérez-Mato (1988) was chosen; the stucture was solved by a least-squares method, using as starting parameters the atomic coordinates of the room-temperature phase of DBCCD previously refined, distorted in the $y$ direction according to the amplitude of the $\Lambda_3$ symmetry mode obtained at 90 K for BCCD (Ezpeleta, Zúñiga, Pérez-Mato, Paciorek & Breczewski, 1992). The origin for this polar structure was defined by software. All atoms were refined with anisotropic displacement parameters and an extinction parameter was included during the last cycles of refinement. $R$ values and goodness-of-fit resulting from the refinements are summarized in Table 2. The atomic parameters of both phases are reported in Table 3.* Selected bond distances and angles are given in Table 4.

A view of the DBCCD molecule at room temperature and a projection of the structure at 35 K are shown in

*Lists of structure factors and anisotropic displacement parameters have been deposited with the IUCr (Reference: HR0028). Copies may be obtained through The Managing Editor, International Union of Crystallography, 5 Abbey Square, Chester CH1 2HU, England.

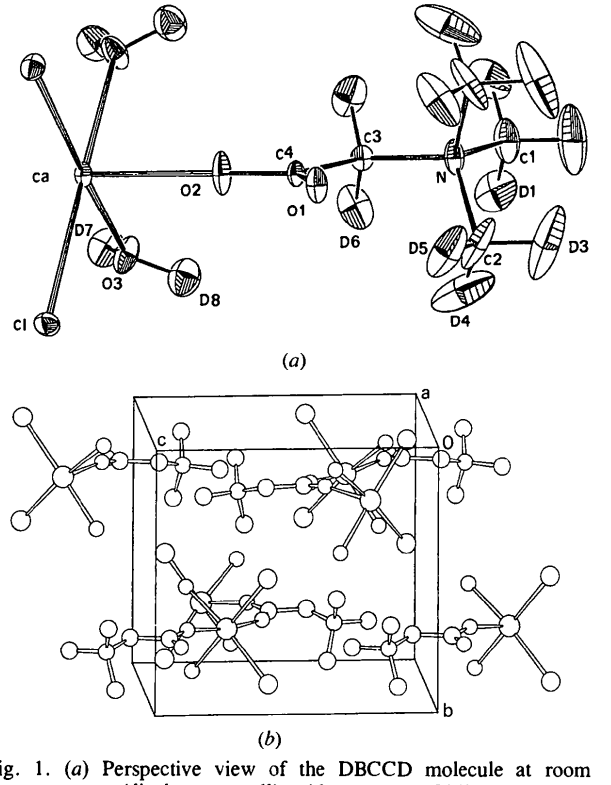


Fig. 1. (*a*) Perspective view of the DBCCD molecule at room temperature (displacement ellipsoids represent 20% probability). (*b*) Projection of the unit cell of the ferroelectric structure of DBCCD at 35 K.

Table 5. *Amplitudes ($\times 10^5$) in units of fractional coordinates of the symmetry modes in the ferroelectric structure*

| | Cl | C2 | O3 | D1 | D3 | D4 | D5 | D6 | D7 | D8 |
|---|---|---|---|---|---|---|---|---|---|---|
| $A_{1g}(x)$ | −86 | 1151 | −100 | 2119 | 1877 | 1394 | 509 | 851 | −437 | −45 |
| $A_{1g}(y)$ | 140 | −280 | 581 | 470 | −373 | 307 | 353 | 397 | 695 | 255 |
| $A_{1g}(z)$ | 17 | 199 | −9 | 1295 | −579 | 308 | −881 | 184 | −25 | 262 |
| $B_{2u}(x)$ | 2418 | −4041 | 2002 | −2855 | −4415 | −7088 | −3499 | −3407 | 2055 | 2099 |
| $B_{2u}(y)$ | −4886 | 4062 | 911 | 638 | 9075 | 1837 | 3179 | −7413 | −905 | −111 |
| $B_{2u}(z)$ | −205 | −2905 | −2095 | −1975 | −2755 | −5344 | −2591 | −1095 | −1165 | −1720 |

| | Ca | O1 | O2 | C1 | C3 | C4 | N | D2 |
|---|---|---|---|---|---|---|---|---|
| $A_{1g}(x)$ | −464 | −288 | −1280 | 1528 | 402 | −482 | 1188 | 2564 |
| $A_{1g}(z)$ | 136 | 92 | 1430 | 1146 | 1318 | 850 | 506 | 732 |
| $B_{2u}(y)$ | −2842 | −3074 | −8148 | 2438 | −5212 | −5278 | 1286 | 7482 |

Fig. 1. Molecules of DBCCD at room temperature are placed on mirror planes and form sheets sharing O atoms (O1) of the carboxyl group. Parallel sheets on planes at $y = 1/4$, $3/4$ are connected through Cl···H—O hydrogen bonds. The lack of the mirror plane at low temperature appears clear; note that Ca—Cl1 and Ca—Cl2 bond distances, which were symmetrically equal in the room-temperature structure, differ now by $\sim 0.02$ Å. The same occurs for the pair Ca—O31 and Ca—O32.

## 3. Symmetry-mode analysis

Our next step was to perform a symmetry mode analysis in order to compare in a quantitative way the structure of the ferroelectric phase with the corresponding ones of the fourfold and the INC phases. In such an analysis the distortion relating the ferroelectric and basic structures is decomposed in terms of symmetry modes of the latter. As this was already done for the fourfold structure, we can follow the behavior of the distortion all along the phase sequence.

The basic procedure of this method is explained in Pérez-Mato, Gaztelúa, Madariaga & Tello (1986). First of all, we determined the symmetry modes contributing to the distortion of the ferroelectric phase, which are $A_{1g}$ and $B_{2u}$ (at $q = 0$). $A_{1g}$ is the fully symmetric representation for the *mmm* point group and $B_{2u}$ is the antisymmetric representation for $C_{2x}$, $C_{2z}$, $I$ and $\sigma_y$. We then obtained the total distortion as a superposition of symmetry modes for each set of symmetry-related atoms in special and general positions of the basic structure of DBCCD. For the eight atoms lying on the mirror plane in the basic structure there are three symmetry mode contributions

$$A_{1g}(x) + A_{1g}(z) + B_{2u}(y).$$

The displacement direction for each mode is indicated in parentheses. For the remaining ten atoms in general positions there are six contributions

$$A_{1g}(x) + A_{1g}(y) + A_{1g}(z) + B_{2u}(x) + B_{2u}(y) + B_{2u}(z).$$

Finally, we performed a Fourier analysis to determine the weight of these modes in the total distortion. The procedure we used in this case is analogous to that presented in Ezpeleta, Zúñiga, Pérez-Mato, Paciorek & Breczewski (1992). To determine the displacement field, we compare the atomic coordinates of the ferroelectric and the room-temperature structures of DBCCD. The results are shown in Table 5. The amplitude of the $B_{2u}$ mode along the $y$ direction should be taken with care, because this mode represents a translation of all atoms along the $y$ direction and the origin of the ferroelectric structure in this direction was chosen arbitrarily due to the polar character of the space group.

## 4. Discussion

Inspection of the atomic displacement ellipsoids of DBCCD at room temperature (see Fig. 1) makes apparent the existence of internal molecule motions, particularly twists of the methyl $CD_3$ groups. We tried to obtain quantitative evidence of these motions by applying a generalization of the **TLS** analysis (Dunitz, Schomaker & Trueblood, 1988), which allows for one additional mean-squared torsional amplitude of each suspected nonrigid group to account for twist motions. We use this treatment only for the group of atoms forming the betaine molecule and at room temperature, fitting the $U_{ij}$ values to an overall rigid-body molecular **TLS** plus three additional mean-squared amplitudes for the twist around parallel axes to the N—C1, N—C2 and N—C3 bonds. The values obtained for the diagonal components of the translational **T** and rotational **L** thermal tensors are $T_{11} = 0.0022(2)$, $T_{22} = 0.034(4)$, $T_{33} = 0.028(3)$ Å$^2$ and $L_{11} = 0.016(2)$, $L_{22} = 0.007(1)$, $L_{33} = 0.037(1)$ rad$^2$, respectively. For the mean-squared internal amplitude values of 0.014(8) and 0.034(6) rad$^2$ for the C1—(D1, D1′, D2), C2—(D3, D4, D5) groups and an unrealistic value of −0.007(7) rad$^2$ for the C3—(D6, D6′, C4) group were found. Among these values, only the second (112°) is meaningful as it is larger than the parallel component of the rotational tensor along the N1—C2 axis. The fit gave an overall $R$ disagree-

Table 6. *Rotations and translations of the different fitted rigid-body groups*

Rotations in sexagesimal degrees and translations ($\times 10^3$) in relative units. $D$ is the agreement factor.

Group 1 = C1—N—C21—C22—C3
Group 2 = C1—N—C21—C22—C3—C4
Group 3 = C1—D11—D12—D2—N—C21—D31—D41—D51—C22—D32—D42—D52—C3
Group 4 = Ca—Cl1—Cl2—O31—O32

| Group | *Rx* | *Ry* | *Rz* | *Tx* | *Ty* | *Tz* | *D* |
|---|---|---|---|---|---|---|---|
| 1 | −7.433 | 1.639 | 10.445 | 5.42 | 6.64 | 3.37 | 0.05 |
| 2 | −6.365 | 1.769 | 10.177 | 4.15 | 1.30 | 3.51 | 0.12 |
| 3 | −7.790 | 2.147 | 10.489 | 6.40 | 9.87 | 2.16 | 0.08 |
| 4 | −2.063 | −0.0286 | −4.126 | −0.824 | −14.4 | 0.175 | 0.28 |

ment factor $U_{ij}$ of 0.098. We have also carried out a **TLS** analysis considering the betaine molecule as a rigid-body unit, resulting in values of $T_{11} = 0.004(2)$, $T_{22} = 0.07(1)$, $T_{33} = 0.024(8)$ Å$^2$ and $L_{11} = 0.024(3)$, $L_{22} = 0.094(1)$, $L_{33} = 0.033(5)$ rad$^2$, respectively, and a fit factor $R$ of 0.15, clearly worse than before. To obtain more insight on the internal molecular motions, an estimation of the **TLS** tensors from a lattice-dynamical model could be very valuable. From this type of calculation the internal mean-squared amplitudes can be unambiguously ascribed to the internal twist of groups nonrigidly attached to the body of the molecule, whereas the similar interpretation from the quantities obtained from the above **TLS** fit may fail due to uncertainty about the relative phases of motions (Dunitz, Schomaker & Trueblood, 1988).

The individual atomic displacements in the low-temperature phase with respect to the basic structure were fitted to a rigid-body model in order to determine the molecular motions involved in the phase transition. This analysis has been performed considering different rigid-body groups with results shown in Table 6. The agreement factor $D$ of the fitting corresponds to the value $[\Sigma(d_c - d_o)^2/\Sigma d_0^2]^{1/2}$, where $d_o$ are the observed atomic displacements and $d_c$ the calculated ones in the rigid-body approximation. The best fit is obtained when the N—C1—C21—C22—C3 group is considered and the agreement decreases considerably when this group is enlarged to include the remaining atoms in the betaine molecule. The deuterium atoms in the methyl groups of the betaine molecule follow the displacements of the C atoms to which they are bonded. The result for the Ca octahedron is worse than for the betaine. It should be stressed that the amplitudes of the rotations of the different atomic groups are similar to those found in the INC structure at 130 K.

Table 5 shows that, in general, the $B_{2u}$ distortion clearly predominates and this is what we could expect from the fact that $B_{2u}$ is the irreducible representation of *Pnma* at $q = 0$, which is compatible with $\Lambda_3$ (the symmetry of the order parameter at $q \neq 0$ all along the phase sequence).

Let us now compare the distortion in the ferroelectric phase with the corresponding ones to the fourfold and INC phases. From the studies of these two phases the eigenvector of the primary distortion, which should correspond to the eigenvector of the soft mode, was determined. By symmetry, this eigenvector for each independent atom must have the following form

$$e_{\Lambda_3} = e_{B_{3g}} + ie_{B_{2u}}.$$

$B_{3g}$ is the antisymmetric representation for $C_{2y}$, $C_{2z}$, $\sigma_y$ and $\sigma_z$. The modulation was then given in terms of the amplitude $|e_{\Lambda_3}|$ for each independent atom and its phase

$$\Phi = \arctan(e_{B_{2u}}/e_{B_{3g}}).$$

Therefore, the term $|e_{\Lambda 3}| \sin \Phi$ of the atomic modulations found in the INC and fourfold phase give

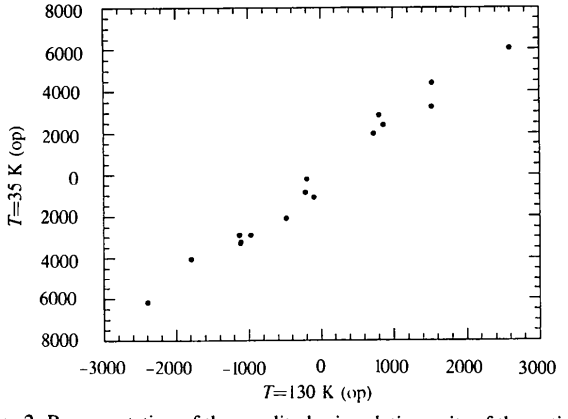


Fig. 2. Representation of the amplitudes in relative units of the optical parts of the $B_{2u}$ modes obtained at 35 K against the corresponding ones in the incommensurate structure at 130 K.

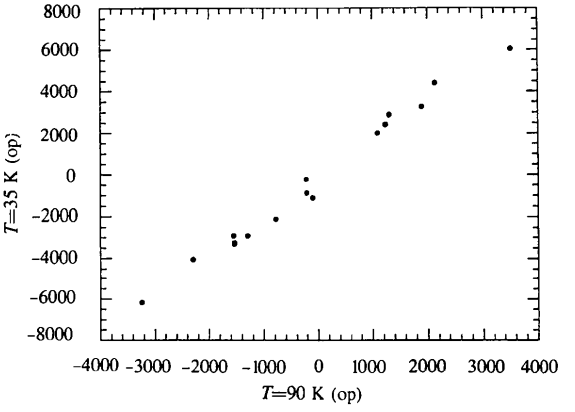


Fig. 3. Representation of the amplitudes in relative units of the optical parts of the $B_{2u}$ modes obtained at 35 K against the corresponding ones in the fourfold structure at 90 K.

the $B_{2u}$ component present in these distortions. Once the $B_{2u}$ distortions were determined for the INC, fourfold and ferroelectric phases, it is still not possible to perform a direct comparison among them due to the arbitrary choice of the origin in the $y$ direction for the ferroelectric phase giving rise to $B_{2u}$ components along the $y$ direction, which have no absolute value. In order to avoid this, the $B_{2u}$ mode was decomposed in its acoustic and optical parts for the three phases. This was carried out using the orthogonality properties of the polarization vectors and taking into account that the optical part of the distortion leaves the center of mass of the cell unchanged. Figs. 2 and 3 show the comparison of the optical part of the $B_{2u}$ mode at different temperatures. A comparison of the 'acoustical' part of the $B_{2u}$ mode in the ferroelectric phase with those in the other two phases has no sense, because in the former case it is arbitrary as it depends on the origin chosen along the $y$ axis.

The two figures are almost identical because of the nearly perfect correlation of the mode $B_{2u}$ at 130 and 90 K used as references in Figs. 2 and 3, respectively. All points in both figures were fitted to straight lines. The slopes of these lines are 2.56 for Fig. 2 and 1.89 for Fig. 3, in accordance with the expected continuous increase of the mode amplitude as the temperature decreases. We can conclude from these results that the structure of the primary mode remains essentially unaltered in the ferroelectric and fourfold or INC structures. There is only a change in its global amplitude as temperature decreases.

The authors wish to thank the Spanish DGICYT and the UPV/EHU for financial support through the projects PB91-0554 and UPV063.310-EBI77/94. JME and FJZ would like to thank I. Etxebarria and J. M. Pérez-Mato for helpful discussions.

## References

Almeida, A., Chaves, M. R., Kiat, J. M., Schneck, J., Schwarz, W., Toledano, J. C., Ribeiro, J. L., Klopperpieper, A., Muser, H. E. & Albers, J. (1992). *Phys. Rev. B*, **45**, 9576–9582.

Brill, W. & Ehses, K. H. (1985). *J. Appl. Phys.* **24**, Suppl. 24-2, 826–829.

Brill, W., Schildkamp, W. & Spilker, J. (1985). *Z. Kristallogr.* **172**, 281–289.

Chaves, M. R., Almeida, A., Toledano, J. C., Schneck, J., Kiat, J. M., Schwarz, W., Ribeiro, J. L., Klopperpieper, A., Albers, J. & Muser, H. E. (1993). *Phys. Rev. B*, **48**, 13318–13325.

Chaves, M. R., Kiat, J. M., Schwarz, W., Schneck, J., Almeida, A., Klopperpieper, A., Muser, H. E. & Albers, J. (1993). *Phys. Rev. B*, **48**, 5852–5856.

Dvorák, V. (1990). *Ferroelectrics*, **104**, 135–146.

Dunitz, J. D., Schomaker, V. & Trueblood, K. N. (1988). *J. Phys. Chem.* **92**, 856–867.

Ezpeleta, J. M., Zúñiga, F. J., Pérez-Mato, J. M., Paciorek, W. A. & Breczewski, T. (1992). *Acta Cryst.* B**48**, 261–269.

Pérez-Mato, J. M. (1988). *Solid State Commun.* **67**(12), 1145–1150.

Pérez-Mato, J. M., Gaztelúa, F., Madariaga, G. & Tello, M. J. (1986). *J. Phys. C*, **19**, 1923–1935.

Ribeiro, J. L., Tolédano, J. C., Chaves, M. R., Almeida, A., Muser, H. E., Albers, J. & Klopperpieper, A. (1990). *Phys. Rev. B*, **41**, 2343–2347.

Sears, V. F. (1992). *International Tables for Crystallography*, Vol. C, edited by A. J. C. Wilson, Section 4.4.4. Dordrecht: Kluwer Academic Publishers.

Stewart, J. M., Kruger, G. J., Ammon, H. L., Dickinson, C. W. & Hall, S. R. (1972). *The XRAY72 System*. Version of June 1972. Technical Report TR-192. Computer Science Centre, University of Maryland, College Park, Maryland, USA.

Tentrup, T. & Siems, R. (1990). *Ferroelectrics*, **105**, 379–384.

Unruh, H. G., Hero, F. & Dvorak, V. (1989). *Solid State Commun.* **70**, 403–408.

Zúñiga, F. J., Ezpeleta, J. M., Pérez-Mato, J. M., Paciorek, W. A. & Madariaga, G. (1991). *Phase Transit.* **31**, 29–43